# CAI DAMAGE MECHANISM CHARACTERISATION

Y. Yang, S. Li

Faculty of Engineering, University of Nottingham
Nottingham NG7 2RD, UK
Email: emxyy2@nottingham.ac.uk

**Keywords:** Damage mechanism, Stress concentration, Delamination propagation, Compression, CAI

## ABSTRACT

Composite laminates have already been used in primary structures of aircrafts. As one of the most important parameters for material selection and structure design, compression after impact [1] strength is conventionally obtained through experiments which are usually expensive and time consuming. For the purpose of reduction of cost and design cycle period, theoretical prediction method of CAI has been pursued over the past decades. However, a widely acceptable prediction method is still not yet available. One of the reasons is that the damage mechanism is not clearly understood. In this paper, a number of characteristic mechanisms of CAI are observed through extensive parametric study, and multiplicity of delamination is considered as the dominating factor: with few and small delaminations close to the mid-plane, laminates usually collapse due to global buckling; with few but big delaminations close to the mid-plane or few delaminations close to either surface, delamination propagates extensively; with moderate numbers of delaminations, delamination propagation may be observed as well as in-plane failure at the delamination front; with large number of delaminations, only in-plane failure are observed. For most CAI cases, large number of delaminations are generated by foreign object impact, and their failure modes are almost ruled in in-plane failure. This conclusion is very helpful for developing a computationally efficient method to predict CAI which only takes in-plane failure into consideration.

## 1 INTRODUCTION

Composite laminates have been successfully used in primary structures of military and commercial airplanes attributing to its superior mechanical properties. However, because of the layered characteristic, laminates is also well known for its susceptibility to foreign object impact, such as dropping tool during the maintenance or runway debris when taking-off and landing. Such impact damage is a serious potential threat to flight safety. One reason is that after impact, large scale of delaminations as well as transverse matrix cracks and fibre breakage are generated which cripple the mechanical properties significantly. Another reason is that such damage usually submerges inside the laminates and is difficult to be detected. This may lead unsuccessful detection of such damage before it develops fatally.

Among impaired mechanical properties due to impact compression behaviour is affected most seriously. Researches reveal up to 60% loss of compressive strength when no obvious defect is observed from exterior [2]. Because the residual compressive strength influences material selection and structure design directly, its significance is always highly concerned and substantial researches were devoted to it in the past three decades. Especially, the impacted laminate bearing barely visible impact damage (BVID) is the most dangerous pattern to continuous fight safety. Therefore, the residual compression after impact [1] strength at this damage level is usually considered as one of the critical values affecting the determination of design value in design process. Currently, the most reliable way to obtain CAI is through excessive experiments which are expensive and time consuming however. Of course, theoretical method to predict CAI was being developed all the time and diverse methods have been presented. Unfortunately, there is not a widely acceptable method so far. One of the reasons is that the damage mechanism of CAI is still not clearly identified.

Damage mechanism of CAI is not easily observed as the development of damage progresses mainly inside the laminates. Although some instruments, such as inferred camera and sound emission,

are able to detect the occurrence of damage inside, they hardly distinguish between different damage modes. C-scan is an especially efficient approach for detecting the delamination distribution and it is employed by many researchers to monitor the delamination-propagating process. Within the author's knowledge, a few cases were reported observing the phenomenon of delamination propagation successfully during the compressing process (Table. 1).

Table 1 Reported cases of delamination propagation (In column "Type", A for artificially induced delamination, I for impact-induced delamination)

| Material system | Referring | Specimen size Length*width (mm*mm) | Lay-up | Delamination | | |
|---|---|---|---|---|---|---|
| | | | | Type | Numbers | Radius (mm) |
| HTA/6376C | Nilsson, Asp [3] | 150*150 | $[(90/0)_{17}/90]$ | A | 3, 5, 7 | 30 |
| IM7/977-2 T800/5245C | De Freitas and Reis [4] | 150*100 | $[-45\_4/45\_4/0\_3/90]_S$ $[-45\_3/45\_3/0\_5/90]_S$ | I | 6 | N/A |
| IM600/133 | Aoki, Kondo [5] | 150*100 | $[45/0/-45/90]_{4S}$ | A | 7 | 8-20 |
| HTA7/6376C | Nilsson, Thesken [6] | 300*150 | $[90/0/90]_{16}$ | A | 15 | 10 |
| HS160/REM | Ruan, Aymerich [7] | 87.5*65 | $[0_3/90_3]_S$ | I | 2 | N/A |

In the meantime, the damage mechanism of CAI is tried to be investigated analytically based on the existing characteristics, for example the presence of large scale of delaminations. One commonly accepted perception of the damage mechanism is delamination propagation. When the delaminated laminate is subjected compressive load, sublaminates lose stability and turn into post-buckling state. Consequently, a tendency of relative movements of neighbouring sublaminates arises, rendering energy release rate (ERR) at delamination front increasing. Therefore, it is natural to associate that once ERR exceeds its critical value, delamination propagation takes place and the whole laminate collapses due to this unstable and catastrophic propagation. Started from this perception, Chai, Babcock [8] presented an analytical model to predict the failure load in which a single one-dimensional delamination or also referred as through-width delamination was assumed. Afterwards, many other researchers continued this research and developed the problem from single delamination to multiple delaminations ([9] [10] [11] [3]). However, in through-width delamination case, the delamination can only propagate along the loading direction which is not in accordance with CAI cases in which failure occurs over the width perpendicular to the loading direction. Therefore, model with two-dimensional delamination is developed. At beginning, the assumption of circular or elliptical delamination is widely adopted due to its relatively less complication for analytical and numerical analysis ([12], [13], [14], [15], [16]). However, experimental evidence proved that circular or elliptical delamination assumption deviates from reality a little bit more and peanut shape or double spiral fan-shape delamination is more appropriate [17], [2], [18], [5], [16]). Additionally, dealing with delamination propagation in CAI case simulation of delamination propagation is not the only intractable issue, geometric nonlinearity with structural instability, the contact problem of multiple interfaces, and the damage growth at multiple sites [15] also need to be considered simultaneously. In this situation, analytical method is almost infeasible and numerical approach such as finite element (FE) method demostrates its powerful applicability. Thanks to the fast developing computation capability and newly developed technology in FE method such as simulating delamination propagation [19], the extremely complex FE model can be analyzed on small-scale workstation or even desktop, and this promotes abundant investigation on this realm in recent years. However, even though, the computation cost is still high and dozens of hours are needed for calculation [17].

On the other hand, although delamination propagation is widely accepted as the damage mechanism of CAI, there are a lot of researchers supporting another viewpoint ([20], [21], [22], [23], [24], [25], [26]). They believed that delaminated area was easy to buckle and could only sustain reduced compressive load afterwards when the impacted laminate was subjected to compression. Therefore, stress redistributed and stress concentration arose around the edge of delaminated area, which led catastrophic failure of the whole plate when the concentrated stress exceeded its strength. An interesting evidence to support this viewpoint is the following. At beginning, engineers endeavoured to increase the matrix toughness of the laminate since they believed this can enhance the fracture toughness to impede potential delamination propagation, and CAI would be increased significantly as a consequence. However, experimental results demonstrated that if the brittle and tough laminate had identical delamination areas due to impact, the CAI values were almost the same [20, 22, 27-29]. This negates delamination propagation as the damage mechanism but supports stress concentration instead. If the viewpoint of stress concentration is tenable, the CAI prediction method can be significantly simplified compared with which based on the perception of delamination propagation. Because the damage mode of delamination propagation is waived, expensive computation cost for simulation of delamination propagation can be saved.

Although these two viewpoints have co-existed for decades, there are few papers found to argue this within author's knowledge. Actually, it is believed that these two damage modes co-exist in the damage process of CAI, and compete mutually to be the dominant damage mechanism based on various factors such as geometry size, boundary condition, material system and impact damage status, etc.. Unfortunately, within the author's knowledge, no public literature is found investigating the damage mechanism through the model which is capable of considering both damage modes simultaneously. A clear understanding of the damage mechanism in diverse circumstances is essential for developing CAI prediction method. With this object, extensive parametric study was conducted on FE models which took both failure modes, delamination propagation and in-plane failure due to stress concentration, into consideration simultaneously. Through this analysis, a number of characteristic mechanisms of CAI are observed and multiplicity of delamination is found as the dominating factor to influence the damage process. Although through the parametric study here cannot reveal the damage mechanism of CAI ultimately because of the idealisation made to these FE models, the knowledge obtained here is profoundly supportive for the damage mechanism investigation further.

## 2 FE MODEL

### 2.1 Construction method

In this paper, all FE models are constructed and analyzed on the ABAQUS platform. Assume there are n initial delaminations present at different position over the laminate thickness. Consequently the laminate is partitioned into (n+1) sublaminates, each of which is meshed with a layer of continuous shell elements. Contact conditions are introduced in the delaminated area in order to avoid impractical interpenetration during deformation. Over the intact part between each two neighbouring sublaminates a layer of zero thickness cohesive elements is introduced for the purpose of simulating potential delamination propagation. A schematic section view of the laminate to illustrate the configuration is demonstrated in Figure 1(a) (delaminated areas are exaggerated for the purpose of clear visibility), in which narrower hatched strips represent initial delaminations and the thicker lines between sublaminates represent interfaces where delamination may propagate through.

The geometry size and boundary conditions are consistent with the requirement of test standard ASTM D7137. The in-plane dimensions of the FE model are 150mm in length and 100mm in width (Figure 1(b)). Compressive displacements are applied on the width edges to simulate the compression load applied by test machine in displacement control mode. The out-of-plane displacement on both width edges is constrained and therefore the width edges can expand freely in width direction due to Poisson's effect when the panel is compressed. Moreover, nodes on the top and bottom surfaces along the lines as shown in Figure 1(b) are constrained for the out-of-plane displacements, representing the two sliding edges aligning with compressive load direction, one on each side approximate 4mm off from the length edge. This constraint is to simulate the anti-global-buckling device which consists of two pairs of slide plates with knife edges as required in the test standard.

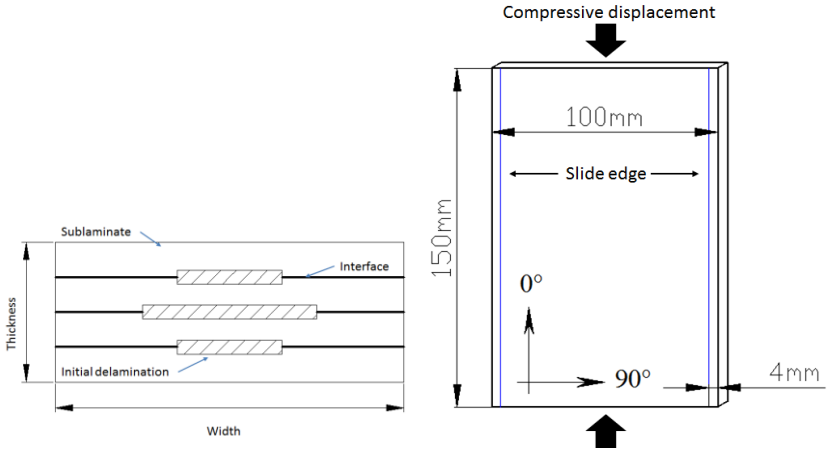


Figure 1 Schematic of (a) section view of delaminated laminate and (b) details of the CAI model

Due to the complication of the FE models, ABAQUS/Explicit is selected as the solver. As CAI test is considered as quasi-static test, the virtual loading speed is set ultimately as total 1.4mm compressive displacement over 1.5s, through careful balancing between precision and computation cost.

Uniform 8-node hexahedron elements are employed for discretizing the laminate model, as shown in Figure 2(a). Continuum shell element SC8R for sublaminate and cohesive element COH3D8 for potential delamination interface, respectively. Although uniform-meshing strategy is not the best economical solution, it is adopted here based on two considerations. The first reason is to provide a common platform for parametric study. In this paper, successive alterations of numbers of layers, sizes and distribution types of initial delaminations have been considered. A common platform provides convenience for comparisons. The second reason is the concern of potential delamination propagation between sublaminates. In some of other publishing, for example, (as shown in Figure 2(b) [30]), only the mesh at initial delamination front was refined. Once delamination propagated beyond this area, mesh became coarse. As simulation of delamination propagation employing cohesive element is sensitive to mesh density, this meshing strategy tended to delay the delamination propagation numerically. The overall process of delamination propagation will be followed if it does take place. Because the location and extent of potential delamination propagation is unknown, it is wise to have a uniform mesh over the entire domain despite the sacrifice of computation efficiency.

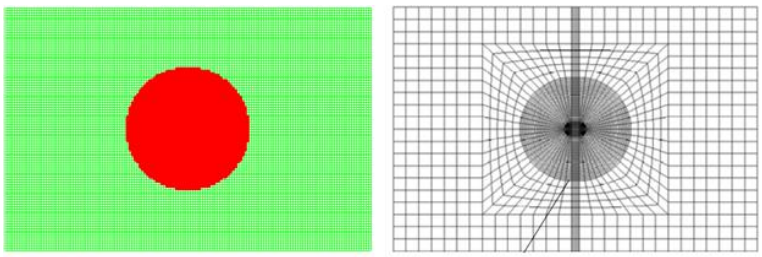


Figure 2 (a) uniform-meshed model (red area represents initial delamination) and (b) an example of partly refined mesh (Fig. 15 from reference 46, shaded circular area represents initial delamination)

As mentioned above, one of the main objective of this paper is to identify which failure mode, delamination propagation or in-plane failure due to stress concentration, is the dominant damage mechanism of CAI. To simulate potential delamination propagation, the built-in power law is employed for cohesive elements, which is expressed in Eq.(1).

$$\frac{G_I}{G_{Ic}} + \frac{G_{II}}{G_{IIc}} + \frac{G_{III}}{G_{IIIc}} \leq 1 \qquad (1)$$

where $G_{Ic}$, $G_{IIc}$ and $G_{IIIc}$ are the critical ERR of Mode I, II and III, respectively, in which $G_{Ic}$ and $G_{IIc}$ have been obtained from relevant experiments, respectively. The value of $G_{IIIc}$ is assigned to be equal to $G_{IIc}$ conventionally.

In order to simulate in-plane failure of individual lamina, a built-in Hashin's failure criterion is employed, which was first presented by Hashin [31]. For brevity, it is not repeated here.

The unidirectional lamina employed in this paper is IM7/8551-7 [32]. The lay-up sequence is [45/0/-45/90]3S, in which fibre orientation is with respect to the x axis demonstrated in Figure 1(b). The reason why only this lay-up sequence is employed is that quasi-isotropic lay-up is widely used in aircraft structure design. Besides, only one type of thickness is employed is because the effect of thickness variation to damage mechanism can be reflected through altering the number of delaminations.

## 2.2 Parametric study coverage matrix

In this paper, the delamination on each interface is assumed to be in a circular shape only, rather than double spiral fan-shape which is closer to reality. Furthermore, other damage modes, such as transverse matrix cracks and fibre breakage, are not taken into consideration. This is because delaminations are considered as the dominance to CAI (Rolfes, Noack [33], Craven [34], Dost [20]), and also the parametric study here does not aim to predict CAI precisely but to investigate the switch of damage mechanism influenced by varying delamination patterns. Therefore, a simplified approach is adopted. However, although the parametric study models represent much simplified idealisation of real CAI cases, some important trends related to the damage mechanisms of CAI can still be revealed and also apply to real CAI problems.

The varying delamination patterns are demonstrated through altering the size, location and number of delaminations. According to these factors the parametric study coverage matrix can be divided into three categories.

In the first category, single delamination, of which the size in terms of radius varies over 10, 15, 20 and 25mm, and the location alters at 4th interface, 8th interface and mid-plane, is considered. It involves 12 cases in this category as listed in Table 2 in terms of FE model names, and the naming rule is illustrated in Figure 3(a).

Table 2 Parametric study coverage matrix of single delamination
(Normal font: Type 1- superfical delamination propagation; **Bold**: Type 2- integral failure)

| | | | |
|---|---|---|---|
| N_1_4_20_R25 | N_1_4_20_R20 | N_1_4_20_R15 | N_1_4_20_R10 |
| **N_1_8_16_R25** | **N_1_8_16_R20** | **N_1_8_16_R15** | **N_1_8_16_R10** |
| **N_1_12_12_R25** | **N_1_12_12_R20** | **N_1_12_12_R15** | **N_1_12_12_R10** |

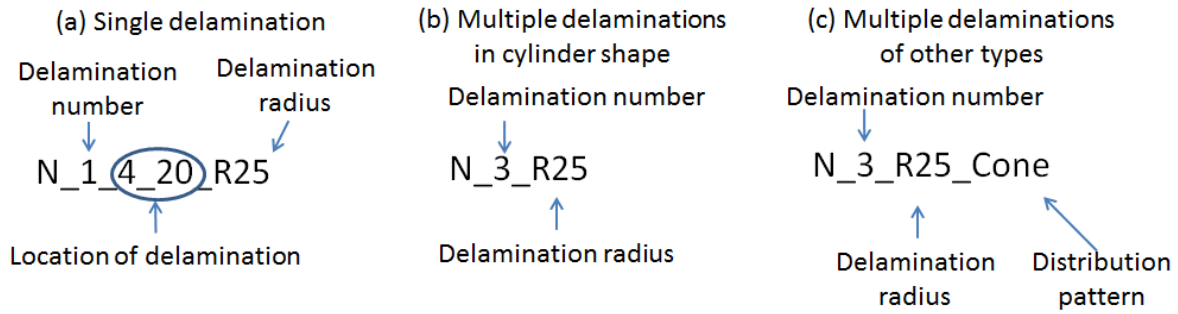


Figure 3 Naming rule of parametric study model of (a) single delamination, (b) multiple delaminations in cylinder and (c) multiple delaminations in other types

In the second category, multiple delaminations are taken into account. The size varies over 15, 20 and 25mm in term of radius, and the number of delaminations varies over 3, 5, 7, 11 and 23. These multiple delaminations are of equal size, evenly spaced through the laminate thickness (Figure 4(a)). It

involves 20 cases in this category as listed in Table 3 in terms of FE model names, and the naming rule is illustrated in Figure 3(b).

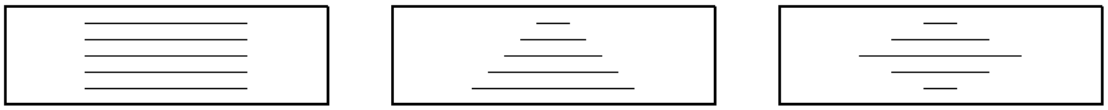


Figure 4 Multiple delaminations distributing in (a) cylinder, (b) cone and (c) spindle shape

Table 3 Parametric study coverage matrix of multiple delaminations in cylinder shape
(*Italic*: Type 3-delamination propagation; ***Bold and italic***: Type 4-stress concentration)

| | | |
|---|---|---|
| *N_3_R25* | *N_3_R20* | *N_3_R15* |
| *N_5_R25* | *N_5_R20* | *N_5_R15* |
| *N_7_R25* | *N_7_R20* | *N_7_R15* |
| ***N_11_R25*** | ***N_11_R20*** | ***N_11_R15*** |
| ***N_23_R25*** | ***N_23_R20*** | ***N_23_R15*** |

Actually, cylinder shape of delamination distribution is less realistic, cone and spindle shapes also need to be considered (Figure 4(b) and (c)). For these patterns, delaminations are still equally spaced but delamination size alters linearly in cone shape and piecewise linearly in spindle shape. The maximum radius varies between 20 and 25mm, while the minimum radius is fixed at 5mm for all patterns. The number of delamination still varies over 3, 5, 7, 11 and 23. Table 4 lists all corresponding FE models and the naming rule is illustrated in Figure 3(c).

Table 4 Parametric study coverage matrix of multiple delaminations in cone and spindle shape
(*Italic*: Type 3-delamination propagation; ***Bold and italic***: Type 4-stress concentration)

| | | |
|---|---|---|
| *N_3_R25_Cone* | *N_3_R20_Cone* | *N_3_R25_Spindle* |
| *N_5_R25_Cone* | *N_5_R20_Cone* | *N_5_R25_Spindle* |
| *N_7_R25_Cone* | *N_7_R20_Cone* | *N_7_R25_Spindle* |
| ***N_11_R25_Cone*** | | ***N_11_R25_Spindle*** |
| ***N_23_R25_Cone*** | | ***N_23_R25_Spindle*** |

## 3 DISCUSSION

After analysing all these FE models mentioned above, it is found that the damage mechanism can be categorised into four types, which are distinguished by font of normal, bold, Italian and bold&Italian in Table 3, 4 and 5, respectively. For brevity, one representative model from each type is selected to illustrate the diverse damage mechanisms. In order to demonstrate the damage process more efficiently, rather than by capturing excessive damage contours from FE model lamina by lamina, an integrated schematic approach is employed. From experiments, as well as simulations, the common catastrophic failure modes of CAI specimens is observed that the specimens tend to break along the centre line across the width where the residual width of intact laminate from the delamination front to the side edge is minimum, leaving two broken halves inserting into each other in a broom shape. Therefore this region deserves more attention for damage mechanism investigation, of which the damage states are reflected in the simplified schematics, for example, Figure 6. The hatched areas indicate initial delamination, grey parts represent interface failure, and black parts represent areas of fibre compression failure. In order to illustrate the damage process, the status of fibre compression failure in the 0° laminae and delamination propagation within the section are captured and shown schematically at a number of critical loading states.

For the first type of damage mechanism, it is characterized with single delamination close to the panel surface and excessive delamination propagation. N_1_4_20_R10 is selected as the representative. Figure 5(a) illustrates the deflection of the central points of both sublaminates during the loading process up to maximum compressive load (referred as failure load in this paper). It is

found that at the beginning, both sublaminates sustain the compressive load together. At about 51.47% failure load, the thinner sublaminate buckles and bends away, while the thicker sublaminate remains stable (the circle in Figure 5(a)). When compressive load reaches 98.49% failure load, a drastic increase of deflection is observed on both sublaminates (the diamonds in Figure 5(a)) due to initiation of delamination propagation. As the compressive load increases, the delamination propagation exacerbates. When failure load is reached, massive delamination is observed, which is shown in the figure on the left of Figure 6(a). However, no fibre failure is observed at the same time. Delamination propagates extensively until fibre failure arises in the thicker sublaminate (figure on the right of Figure 6(a)), and the whole laminate collapses immediately soon.

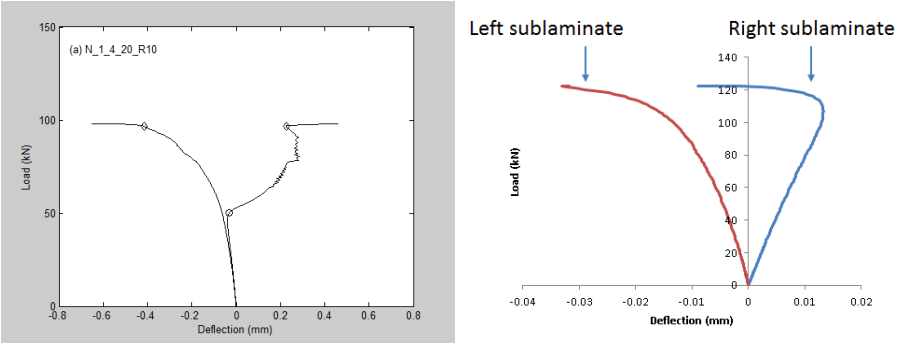


Figure 5 Deflection of central point of FE model (a) N_1_4_20_R10 and (b) N_1_12_12_R20 in loading process

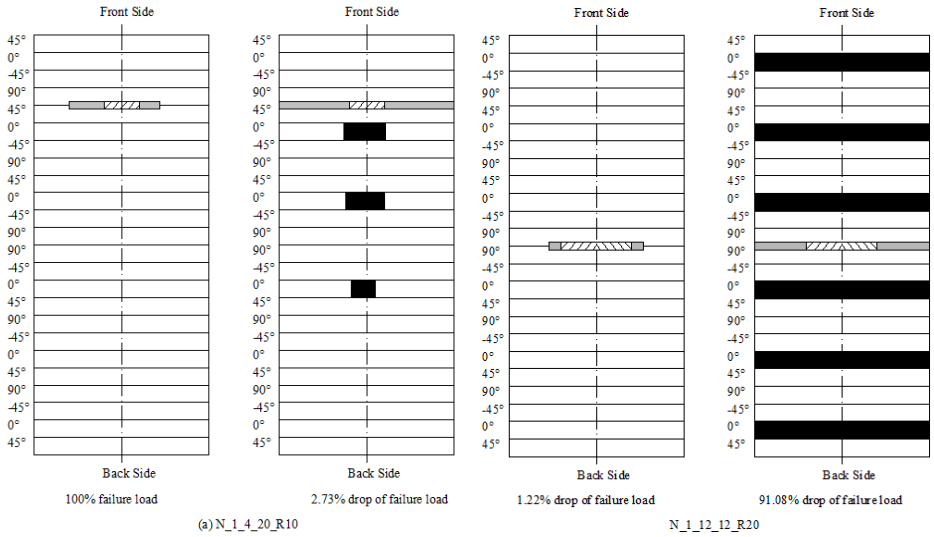


Figure 6 Schematic damage process of (a)N_1_4_20_R10 and (b)N_1_12_12_R20

The second type is characterised by few delaminations and integral collapse. N_1_12_12_R20 is selected as the representative. Figure 5(b) demonstrates the deflection of the central points of both sublaminates up to failure load. It is found that both sublaminates keep stable from the beginning up to 87.6% failure load, then they bend abruptly towards a common direction due to global buckling. The severe bending deformation leads compressive stress in the inner sides of the sublaminates exceeding strength limit rapidly and the whole laminate collapses integrally, which is shown in the figure on the right of Figure 6(b). Although before collapse tiny delamination propagation is observed, about 7mm on each side, which is shown in the figure on the left of Figure 6(b), it has insignificant effect to the ultimate failure mode.

The third type is characterised by moderate number of delaminations and large scale of delamination propagation before collapse. Take N_5_R20 for example, when sublaminates buckle due to the in-plane compression, delamination propagation is triggered, such as shown in the figure on the

left of Figure 7(a). In the meantime, buckling also lead stress redistribution and stress concentration arises at the delamination front. As delamination propagates, concentrated stress increases at the moving delamination front until exceeding strength limit. After that, fibre failure takes place and develops rapidly over the residual intact part along width direction (figure on the right of Figure 7(a)). Consequently, the whole laminate collapses.

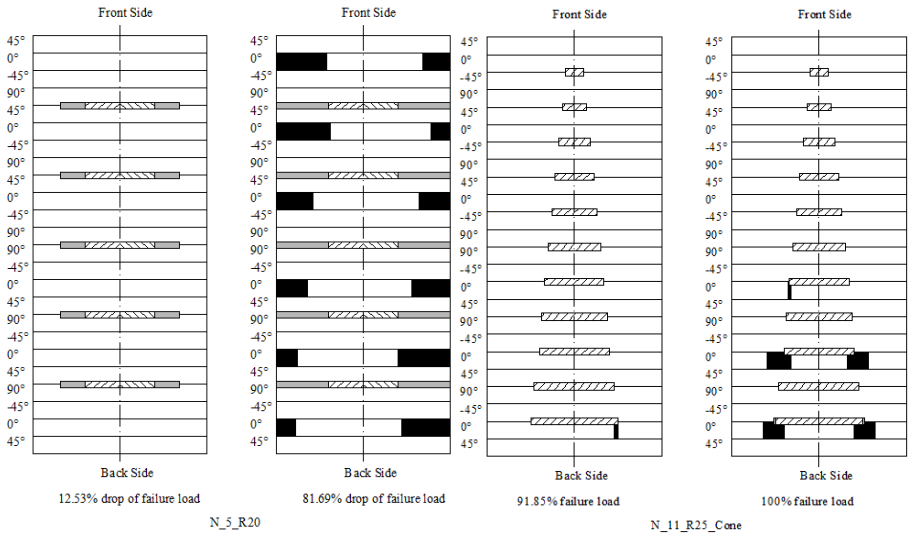


Figure 7 Schematic damage process of (a) N_5_R20 and (b) N_11_R25_Cone

The last type is characterised by the presence of excessive delaminations and fibre failure initiating at original delamination front. Similar to previous type, sublaminates also buckle due to in-plane compression. However, delamination propagation is hard to be triggered before fibre failure due to stress concentration initiating at delamination front. Fibre failure develops along the width direction and the whole laminate collapses. As an example, the damage process of N_11_R25_Cone is shown in Figure 7(b).

Figure 8 shows the diverse ratios of average compressive stress in $0^\circ$ laminae with respect to the compressive strength of the lamina along centre line along the width at the failure load, including all models in Table 3 as well as the models bearing single delamination in the mid-plane in Table 2. It can be found that for the models with single or three delaminations the stress distributes relatively evenly in the undelaminated part and slightly drops at the delaminated area. This is because the plate, although delaminated, sustains the compressive load as an integral. However, as the number of delaminations increases, the overall stress level drops but stress concentration becomes more and more significant at delamination front. Combined with observation from previous investigation, this phenomenon implies that stress concentration is gradually becoming the dominant factor influencing the damage mechanism as the number of delaminations increases.

The failure loads of all models in this group as well as the model bearing single delamination in the mid-plane are compared using a bar chart in Figure 9. An interesting phenomenon is that the failure load doesn't decrease monotonously as the number of delamination increases. Instead, it drops sharply first then rebounds a little at increased number of delaminations. Combined with previous investigation of damage mechanism, it is found that these relatively low failure loads are due to large scale of delamination propagation. In another word, without delamination propagation, the laminate is able to sustain relatively higher compressive load even with more delaminations. In the meantime, it suggests the existence of a specific number of delaminations, neither the fewest nor the most, at which delamination propagation is most likely to take place. This is because ERR, which dictates the delamination propagation, is completely a local factor at the delamination front determined by a couple of factors such as overall compressive load, deformation of sublaminates, the bending rigidity of sublaminates, etc.. Generally, the thicker the sublaminate, the higher the bending rigidity, and the higher ERR accumulated at delamination front when sublaminates bend. However, when there are only few delaminations, the sublaminates are too rigid which leads them retain stable up to relatively

high compression load. Once they buckle, the in-plane compression stress exceeds the strength limit rapidly, causing the whole laminate to collapse abruptly, like the model bearing single delamination at mid-plane or eighth interface in this paper. When there are excessive delaminations, for example, 11 or 23 delaminations in this paper, the bending rigidity of sublaminates are undermined significantly due to its weak thickness. Although sublaminates bend severely, it cannot accumulate sufficient ERR at the delamination front to trigger propagation before the concentrated stress at delamination front exceeds its strength limit to trigger in-plane failure. When there are moderate number of delaminations, the sublaminates can buckle locally to accumulate sufficient ERR for delamination propagation, like the model bearing 5 or 7 delaminations here. That is why it is concluded that when laminate bears moderate number of delaminations, delamination propagation is most likely to take place.

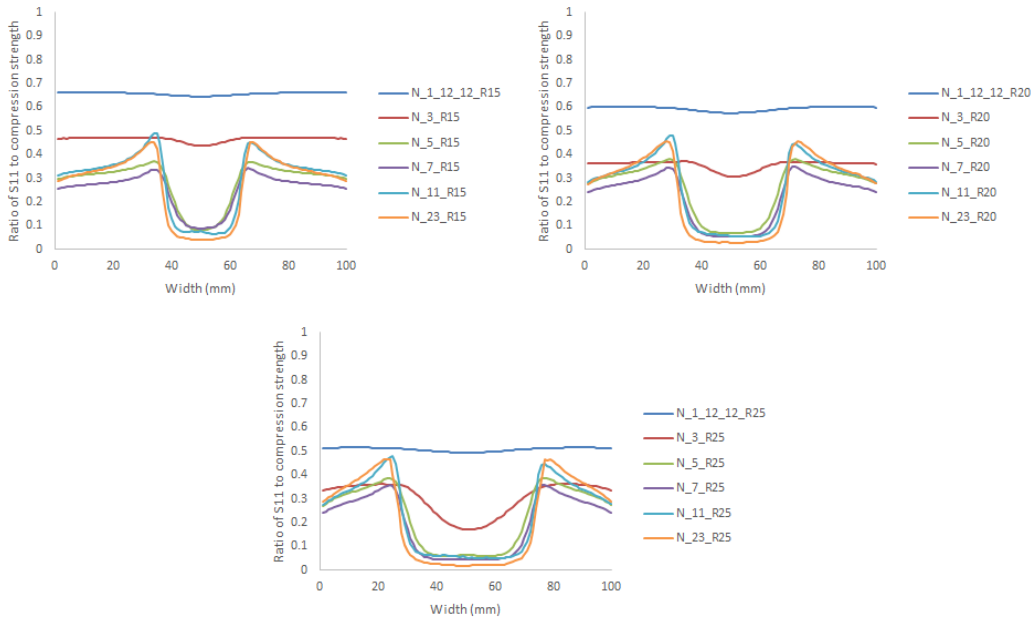


Figure 8 The ratio of compressive stress in 0° laminae to compressive strength over the laminate width at failure load among models of common delamination size ((a) R=15mm, (b) R=20mm, (c) R=25mm) but different numbers of delaminations

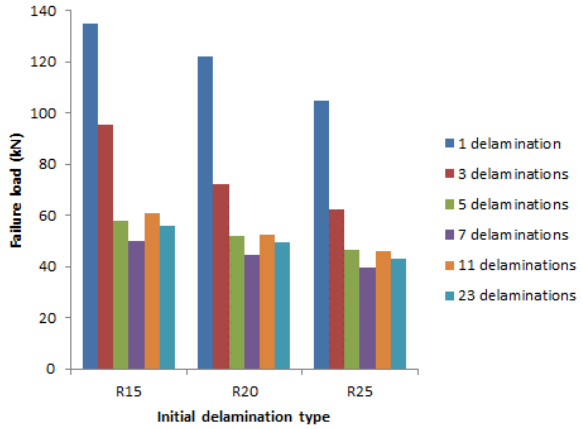


Figure 9 Comparison of failure load of FE models bearing multiple delamination

## 4 SUMMARY

Results through above analysis reveal that the development of CAI damage shows a number of characteristic mechanisms and the multiplicity of delamination is believed to be the critical factor to dictate the form of the CAI damage mechanisms (Fig. 12). With few and small delaminations close to the mid-plane of the impacted plate, laminates usually collapse as an intact plate due to loss of stability. With few delaminations close to the surface, or few but big delaminations close to the mid-plane, delamination may propagate extensively. With moderate number of delaminations, delaminations propagate to some extent but in-plane failure due to stress concentration lead final collapse. With large number of delaminations, in-plane failure due to stress concentration will lead final collapse of laminates and delamination propagation is unlikely to take place.

This conclusion partially explains the experimental observation of delamination propagation in Table 1. In these reported cases, sublaminates consist of at least 2 or 3 laminae. Therefore, the buckling deformation of these sublaminates is capable to generate adequate ERR at the delamination front for propagation. However, for laminates used in aircraft structure, successive lay-up of laminae with same fibre orientation is usually avoided, leaving a large number of interfaces existing through laminate thickness. Once the laminates are subjected to foreign object impact, a large number of delaminations will be generated, leading the bending rigidity of each sublaminate relatively low. Additionally, transverse matrix crack and fibre breakage due to foreign object impact will impair the bending rigidity further. Therefore, it is reasonable to expect that for most CAI cases in-plane failure due to stress concentration is the dominant damage mechanism and delamination propagation is unlikely to take place in large scale. This conclusion is very helpful for developing a computationally efficient method to predict CAI which takes in-plane failure into consideration only.

## 5 CONCLUSIONS

Damage mechanism of CAI is investigated through extensive parametric study using FE models which take both damage modes, delamination propagation and in-plane failure, into consideration. Results show a number of characteristic mechanisms, which are mainly dictated by the multiplicity of delaminations. It suggests that there exists a threshold of characteristic number of delaminations for a given laminate over which delamination propagation will not take place and in-plane failure due to stress concentration leads final collapse of entire laminate. For most laminates used for aircraft structures, large number of delaminations are generated after foreign object impact. In this situation the damage mechanism of CAI is mainly in-plane failure due to stress concentration, and delamination propagation is unlikely to take place. This conclusion is very helpful for developing a computationally efficient method to predict CAI which only takes in-plane failure into consideration.

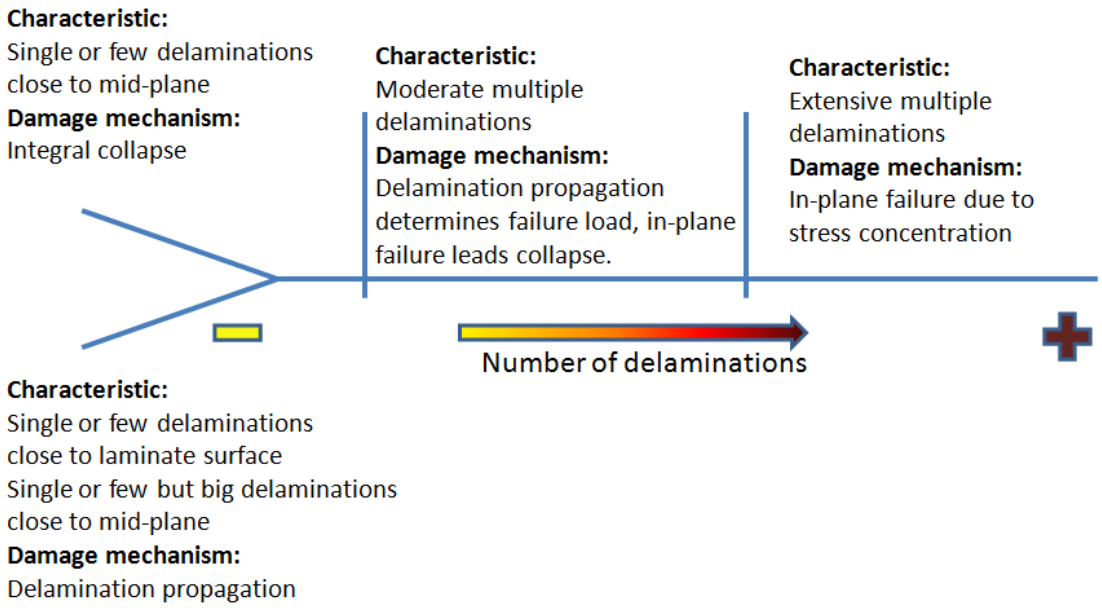

Fig. 12. Schematic partition of damage mechanism of CAI

## ACKNOWLEDGEMENT

The first author wishes to acknowledge the PhD studentship offered by AVIC, China and China Scholarship Council.

## REFERENCE

[1]. Yan, L., et al., *Study on Damage Equivalence of Composite Laminates Subjected to Low-velocity Impact and Quasi-static Indentation.* Journal of Aeronautical Materials, 2011. **31**(3): p. 5.

[2]. Craven, R., L. Iannucci, and R. Olsson, *Delamination buckling: A finite element study with realistic delamination shapes, multiple delaminations and fibre fracture cracks.* Composites Part A: Applied Science and Manufacturing, 2010. **41**(5): p. 684-692.

[3]. Nilsson, K.F., et al., *Delamination buckling and growth for delaminations at different depths in a slender composite panel.* International Journal of Solids and Structures, 2001. **38**(17): p. 3039-3071.

[4]. De Freitas, M. and L. Reis, *Failure mechanisms on composite specimens subjected to compression after impact.* Composite Structures, 1998. **42**(4): p. 365-373.

[5]. Aoki, Y., H. Kondo, and H. Hatta, *Effect of delamination propagation on mechanical behaviour in compression after impact.* ICCM16, Kyoto, Japan, 2007.

[6]. Nilsson, K.F., et al., *A theoretical and experimental investigation of buckling induced delamination growth.* Journal of the Mechanics and Physics of Solids, 1993. **41**(4): p. 749-782.

[7]. Ruan, J., et al., *Optical Evaluation on Delamination Buckling of Composite Laminate with Impact Damage.* Advances in Materials Science and Engineering, 2014. **2014**.

[8]. Chai, H., C.D. Babcock, and W.G. Knauss, *One dimensional modelling of failure in laminated plates by delamination buckling.* International Journal of Solids and Structures, 1981. **17**(11): p. 1069-1083.

[9]. Simitses, G., S. Sallam, and W. Yin, *Effect of delamination of axially loaded homogeneous laminated plates.* AIAA journal, 1985. **23**(9): p. 1437-1444.

[10]. Suemasu, H., *Effects of multiple delaminations on compressive buckling behaviors of composite panels.* Journal of Composite Materials, 1993. **27**(12): p. 1172-1192.

[11]. Lee, J., Z. Gürdal, and O. Griffin Jr, *Buckling and postbuckling of circular plates containing concentric penny-shaped delaminations.* Computers & structures, 1996. **58**(5): p. 1045-1054.

[12]. Whitcomb, J.D. and K. Shivakumar, *Strain-energy release rate analysis of plates with postbuckled delaminations.* Journal of Composite Materials, 1989. **23**(7): p. 714-734.

[13]. Whitcomb, J.D., *Analysis of a laminate with a postbuckled embedded delamination, including contact effects.* Journal of Composite Materials, 1992. **26**(10): p. 1523-1535.

[14]. Reeder, J.R., et al., *Postbuckling and growth of delaminations in composite plates*, 2002, AIAA.

[15]. Suemasu, H., et al., *A numerical study on compressive behavior of composite plates with multiple circular delaminations considering delamination propagation.* Composites Science and Technology, 2008. **68**(12): p. 2562-2567.

[16]. Ovesy, H., M. Taghizadeh, and M. Kharazi, *Post-buckling analysis of composite plates containing embedded delaminations with arbitrary shape by using higher order shear deformation theory.* Composite Structures, 2012. **94**(3): p. 1243-1249.

[17]. Craven, R., L. Iannucci, and R. Olsson, *Homogenised non-linear soft inclusion for simulation of impact damage in composite structures.* Composite Structures, 2011. **93**(2): p. 952-960.
[18]. Suemasu, H., et al. *Compressive behavior of impact damaged composite laminates*. in *In Proc. 16th Int. Conf. on Composite Materials, Kyoto, Japan 8â€“13 July 2007*. 2007.
[19]. Zou, Z., S. Reid, and S. Li, *A continuum damage model for delaminations in laminated composites.* Journal of the Mechanics and Physics of Solids, 2003. **51**(2): p. 333-356.
[20]. Dost, E., *Effect of stacking sequence on impact damage resistance and residual strength for quasi-isotropic laminates*, in *American society for testing and materials*1991: Philadelphia.
[21]. Tang, X. and J. Liu, *Theory manual of CDTAC 1.0*, 1998, Aircraft Strength Research Institute.
[22]. Chen, P., Z. Shen, and J. Wang, *A new method for compression after impact strength prediction of composite laminates.* Journal of Composite Materials, 2002. **36**(5): p. 589-610.
[23]. Soutis, C. and P.T. Curits, *Prediction of the post-impact compressive strength of cfrp laminated composites.* Composite science and technology, 1996. **56**: p. 677-684.
[24]. Xiong, Y., et al., *A prediction method for the compressive strength of impact damaged composite laminates.* composite structures, 1995. **30**: p. 357-367.
[25]. Qi, B. and I. Herszberg, *An engineering approach for predicting residual strength of carbon/epoxy laminates after impact and hygrothermal cycling.* Composite Structures, 1999. **47**(1–4): p. 483-490.
[26]. Nilsson, E., *Residual Strength Prediction of Composite Laminates Containing Impact Damage.* Interface, 2005. **6**(7): p. 8.
[27]. Dost, E.F., et al., *Effect of stacking sequence on impact damage resistance and residual strength for quasi-isotropic laminates*. Composite materials: fatigue and fracture ed. T.K. O'Brien. Vol. 3. 1991, Philadelphia: American society for testing and materials. 24.
[28]. Yang, X., et al., *New methodology for evaluating toughness of composite laminates-investigation of damage resistance.* Chinese Journal of Aeronautics, 2003. **16**(2): p. 73-79.
[29]. Guild, F.J., J.C. Prichard, and P. Hogg, *A model for the reduction in compression strength of continuous fiber composites after impact damage.* Polymer composites, 2001. **24**(4): p. 333-339.
[30]. Suemasu, H., et al. *Compressive behavior of impact damaged composite laminates*. in *In Proc. 16th Int. Conf. on Composite Materials, Kyoto, Japan 8â 13 July 2007*. 2007.
[31]. Hashin, Z., *Failure criteria for unidirectional fiber composites.* Journal of applied mechanics, 1980. **47**(2): p. 329-334.
[32]. Soden, P., M. Hinton, and A. Kaddour, *Lamina properties, lay-up configurations and loading conditions for a range of fibre-reinforced composite laminates.* Composites Science and Technology, 1998. **58**(7): p. 1011-1022.
[33]. Rolfes, R., et al. *Fast Analysis Tools for Concurrent/Integrated Engineering of Composite Airframe Structures*. in *Optimization in Industry...: Presented at the Conference, Optimization in Industry*. 2001. American Society of Mechanical Engineers.
[34]. Craven, R., *Modelling of impact damage in composites*, 2009, Imperial College London.